Proceedings of CONF-MSS 2026 Symposium: Advanced Composite Materials and Polymer Chemistry
DOI: 10.54254/2755-2721/2026.AD33186

Analysis of the Aerodynamic Performance of the NACA0012 Airfoil at Different Reynolds Numbers

Yida Wang

Institute of JEI, Harbin Engineering University, Harbin, China
2023282110@hrbeu.edu.cn

Abstract. With the fast evolving low-altitude economy and green energy, NACA0012 airfoil has gained increased significance in the engineering practice due to its outstanding aerodynamic performance in the field of flow. In order to solve practical needs and problems in micro air vehicles, unmanned aerial vehicles and small wind turbine blades in high Reynolds number regime, this paper employs numerical simulation methods of Computational Fluid Dynamics (CFD) to perform systematic study about aerodynamic performance of NACA0012 airfoil in Reynolds number regime of 560, 000 to 2, 800, 000. Aerodynamic data of the lift, drag at different Angles of Attack (AoA) and Reynolds number was obtained by formulation of digital models and simulation calculations and the laws of influence of the AoA and Reynolds number on the aerodynamic performance of the airfoil were plotted systematically. The range of Reynolds number and conditions of AoA are much more detailed in the paper than in the current research works and thus the parameter space is much more complete. The results of the calculation obtained are rather good in correspondence with the existing research tendencies in literature that proves the universality and reliability of the numeric model used. The results of the study might be applied to justify theoretical backgrounds and information on the design and optimization of low-speed aerodynamic models such as small unmanned aerial vehicles, micro air vehicles, and small wind turbines.

Keywords: NACA0012 airfoil, high Reynolds number, aerodynamic performance

1. Introduction

Aerodynamics refers to the study of forces that are exerted on objects in motion by gases, usually air. It is very important in designing spacecrafts and using wind energy. The NACA series of airfoils constitute a group of airfoil standards created and researched by NASA. Because of their repeatability and comparability, they have turned out to be significant vectors of several aerodynamic applications, offering both theoretical and experimental bases of the optimization of aerodynamic performance and enhancement of structural designs. The NACA0012 airfoil is one of them, and it has a relatively stable aerodynamic performance due to the shape and its symmetry, which is easy to manufacture, which, in turn, makes it widely used in small power devices and micro air vehicles.

© 2026 The Authors. This is an open access article distributed under the terms of the Creative Commons Attribution License 4.0 (https://creativecommons.org/licenses/by/4.0/).

DOI: 10.54254/2755-2721/2026.AD33186

Over the past years, the NACA0012 airfoil has been the subject of a large amount of scholarly research. To research the airfoil's aerodynamic properties, the k-ω SST turbulence model was used by Ayat et al. to simulate the NACA0012 and examined both lift and drag coefficients of the airfoil at four different number of value of Reynolds numbers [1]. Different Angles of Attack (AoA) were also contained to ascertain the effect of the Reynolds number's small variation on the aerodynamic characteristics of the airfoil and the effect of the AoA on T. Jardin et al. experimented the NACA0012 airfoil at Reynolds number from 5e4 to 1.4e5, where the flow characteristics around the NACA0012 airfoil are obtained through experimental and high and low-precision numerical simulation techniques [2]. Numerical simulations on the NACA0012 in full stall were performed by Rodriguez [3]. Mohamad, F et al. also employed Computational Fluid Dynamics (CFD) simulation techniques in comparing and analyzing the performance dissimilarity and the flow characteristics of the NACA0012 airfoil when wavy leading edges and horizontal leading edges are used [4]. Qian Yu et al. applied the numerical calculation technique of dynamic mesh technology to investigate the dynamic stall issue of the NACA0012 [5]. L. Goyaniuk et al. also investigated the flutter phenomenon following the stall of the airfoil [6]. Rak A et.al tested the NACA0012 by experimenting and LBM analysis [7]. Concentrating on the separated flow, large-eddy simulation was used by A. Wang et. al. to find the characteristic of vortices around the airfoil [8].

Previous studies often focused on specific operating conditions, had a relatively narrow Reynolds number range, and insufficient angle precision. Therefore, the main purpose of this paper is to calculate and simulate the aerodynamic performance of the NACA0012 airfoil under various conditions for practical reference. Thus, for Reynolds numbers ranging from 560,000 to 2,800,000, the environment of NACA0012 was analyzed, covering a wider Reynolds number range and more detailed angles, to explore their effects on aerodynamic performance. This simulation study of the airfoil provides certain reference value and also offers data for engineering design in practical applications.

2. Numerical model

2.1. Geometric modeling

Figure 1 presents the geometric model of the NACA0012 airfoil, with the chord length being c = 1000mm. Figure 2 establishes a "C"-shaped fluid domain ranging from 15 c. The length from the center of the airfoil to the end of the computational domain is 15 c, and the diameter of the sectoral area is 15c. In the figure, the front and upper parts of the "C" shape are the velocity base inlets, and the end is the pressure base outlet. This paper selects the "C"-shaped computational domain and the two-dimensional structured grid for the generation of the computational domain and the airfoil grid. The computational domain is divided into 6 sub-regions to better simulate the fluid movement situation. After dividing the computational domain, the meshing is carried out as shown in Figure 3. In the figure, it specifically presents the biased mesh settings with dense grids near the airfoil and sparse grids away from the airfoil. Additionally, the number of partitions in each region is 300, and they are biased with a bias factor of 40000. The entrance, exit, wall, and fluid domain are set.

DOI: 10.54254/2755-2721/2026.AD33186

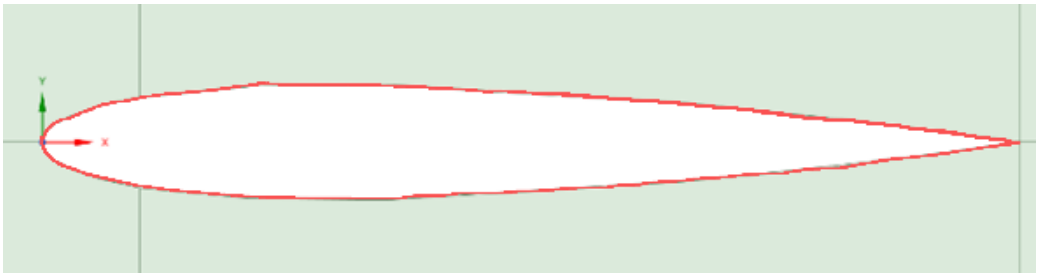


Figure 1. Modeling of NACA0012 airfoil. (picture credit: original)

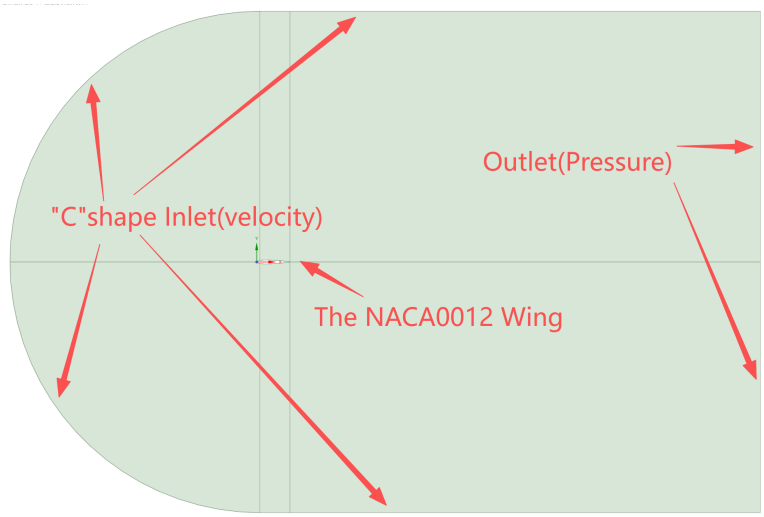


Figure 2. "C"-shaped computational domain and its segmentation. (picture credit: original)

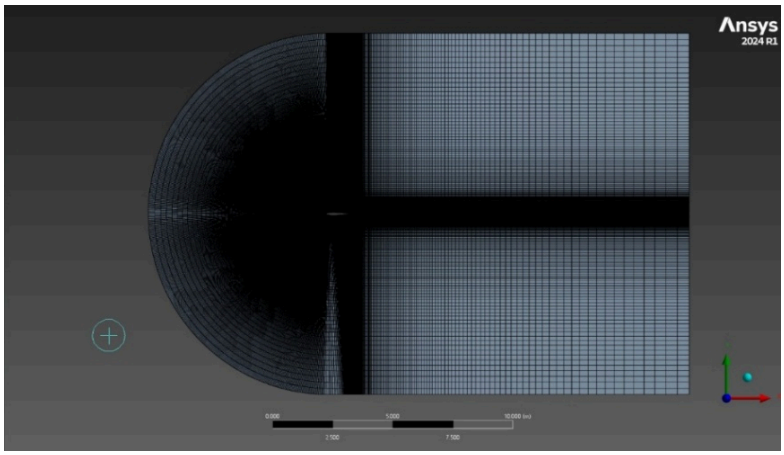


Figure 3. Grid partitioning. (picture credit: original)

2.2. Simulation environment setup

In the simulation, the specific simulation environment settings are shown in Table 1. Additionally, considering the air density at a humidity level of 60% and the height at 1 km, it is set to 1.0 kg/m³. These settings not only have strong practical reference significance but also can extend the low Reynolds number range.

DOI: 10.54254/2755-2721/2026.AD33186

Table 1. CFD simulation calculation parameters

Parameters	Settings
Turbulence Model	K- ω SST Model
Density (kg/m3)	1.0
Viscidity ($\mathrm{kg/m \bullet s}$)	1.7894e-5
Ratio of Turbulent Viscosity	0.1
Intensity of Turbulence	0.05
Inlet Velocity(m/s)	10-50
Reynolds Number	560000-2800000
flux	Second-order windward effect
Pressure-velocity coupling method	Coupled

2.3. Equations of calculation

Mathematical methods for fluid simulation mainly include the continuity equation and the Stokes equation [9,10]. Among them, the continuity equation is shown as Equation (1).

$$\frac{\partial \rho}{\partial t} + \frac{\partial \rho u}{\partial x} + \frac{\partial \rho \mathrm{v}}{\partial \mathrm{y}} + \frac{\partial \rho \mathrm{w}}{\partial \mathrm{z}} = 0 \tag{1}$$

Where ρ represents the density of the fluid; u, v, and w are the velocity components in the x, y, z directions respectively.

Navier-Strokes equation is shown as equation (2).

$$\rho \frac{\partial \mathbf{V}}{\partial t} + \rho\left((\mathbf{V}\cdot)\nabla\right)\mathbf{V} = -\nabla p + \nabla \bullet \left\{\mu\left[\nabla \bullet \mathbf{V} + (\nabla \mathbf{V})^T - \frac{2}{3}\left(\nabla \bullet \mathbf{V}\right)I\right]\right\} \tag{2}$$

Where $\mathbf{V}$ represents the fluid velocity vector; p is the static pressure of the fluid; g is the gravitational acceleration.

The lift coefficient (C_L) and the drag coefficient (C_D) are shown in Equations (3) and (4).

$$C_L = \frac{F_L}{1/2\rho V^2 A} \tag{3}$$

$$C_D = \frac{F_D}{1/2\rho V^2 A} \tag{4}$$

Where F_L and F_D are forces of lift and drag; A represents as the area.

3. Results and discussion

By obtaining the convergent solution through iteration, the C_L , C_D and pressure contour can be output, thereby enabling the analysis of the aerodynamic performance of the wing.

DOI: 10.54254/2755-2721/2026.AD33186

3.1. Analysis of pressure contour

The pressure that is spread across the outer surface of the NACA0012 airfoil at the fluid is denoted on the image on the cloud as observed in Figure 4. This variation in pressure between the obverse and reverse surfaces of the airfoil is the greatest contribution to the C_L as the AoA and Reynolds number varies as observed in the figure. The cloud image also shows the vortices of the obverse and reverse surfaces of the airfoil which can again be studied to derive the moment due to the pressure on the airfoil and incidentally it can also assist in the further study of its aerodynamic performance in detail.

The pressure distribution on the NACA0012 wing surface on the outcome of this study has some physical peculiarities and depends on different AoA.

In this case at low angle the forces on the lower and upper surfaces of the airfoil are equal and the C_L is almost zero. The steeper the AoA, the greater is the deflection of the fluid at the leading edge of the airfoil, and the velocity of flow at the upper surface. According to this law of Bernoulli, the pressure in this area is lower and this forms a distinct zone of low pressure (in blue). Meanwhile, the bottom pressure is high side. It is the major cause of lift due to the difference in pressure between the obverse and reverse surfaces.

As the AoA is further increased (Figure 4 (c)) the region of low pressure in the rear portion of the upper surface begins to expand to the front and its shape is distorted. This means that fluid kinetic energy within the boundary layer is insufficient to counter pressure gradient that is accelerating the separation of large scale flow field to form vortices. This is directly attributed to the worsening of the aerodynamic characteristics of the airfoil.

The massive vortex pattern at the leading edge of the airfoil as denoted in the figure has a strong bearing on the lift and drag.

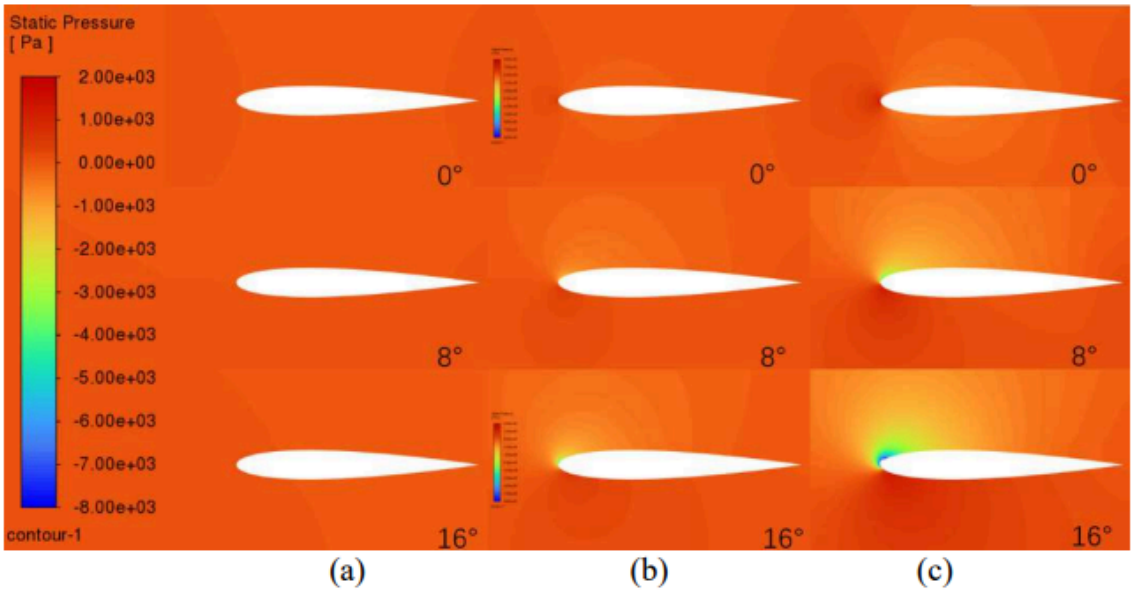


Figure 4. Pressure contour, (a) Re=5.6 × 10^5; (b) Re=1.7 × 10^6; (c) Re=2.8 × 10^6. (picture credit: original)

DOI: 10.54254/2755-2721/2026.AD33186

3.2. The influence of reynolds number on C_L and C_D

This study achieved changes in the Reynolds number by setting different inflow velocities. For each AoA, five sets of different Reynolds numbers, namely 5.6×10^4 , 1.1×10^5 , 1.7×10^5, 2.2×10^5 , 2.8×10^5 were simulated. The simulation results are shown in Figures 5 and 6. Overall, the C_L and C_D of the airfoil show a positive correlation with the Reynolds number. The increase in the C_L is significant, while the increase in the C_D is small, and the fluctuation range of the C_D is much smaller than that of the C_L . Moreover, the change in the C_D is extremely small at low AoA.

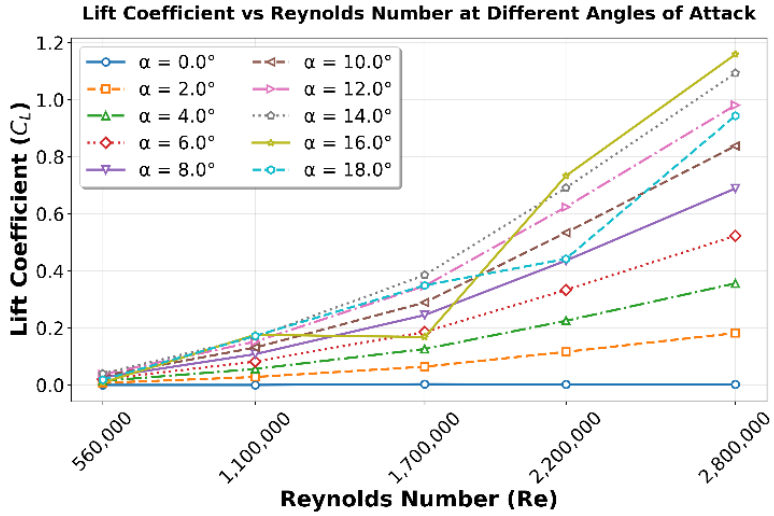


Figure 5. Curves showing the variation of C_L with Reynolds number at different AoA. (picture credit: original)

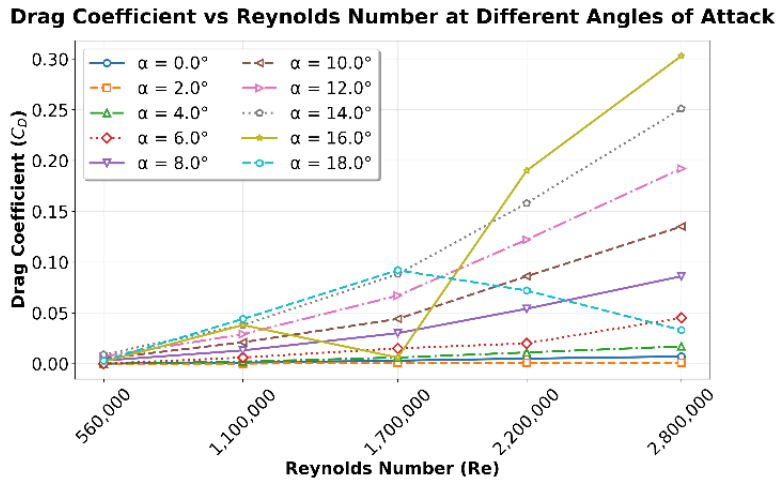


Figure 6. Curves showing the variation of C_D with Reynolds number at different AoA. (picture credit : original)

3.3. The influence of AoA on C_L and C_D

This paper achieves the simulation of different angle-of-attack conditions by changing the component velocities in the X and Y directions of the incoming flow.

DOI: 10.54254/2755-2721/2026.AD33186

To provide more detailed guidance for the structural design, this paper studied the aerodynamic performance within the angle range of 0°-18°, with a step size of 2°. The results are shown in Figures 7 and 8.

According to the simulation outcomes, the range of the AoA can be approximately split into two regions, which are the linear growth region and the stall region. In the linear growth zone, C_L varies linearly with the AoA. At this point the force state of the wing is steady and the fluid moves very near the wing surface. At AoA steeper at 16° there exists a strong inflection point in the curve and the C_L starts to fall off, taking the C_D directly into chaos. This effect signifies that the wing has moved into the stall condition. The zone of separation of the upper surface has now assumed the supreme position. Lift fluctuations are particularly stronger before and after stall at higher Reynolds numbers which is an indication that the wing is more sensitive to variations in the AoA at high Re.

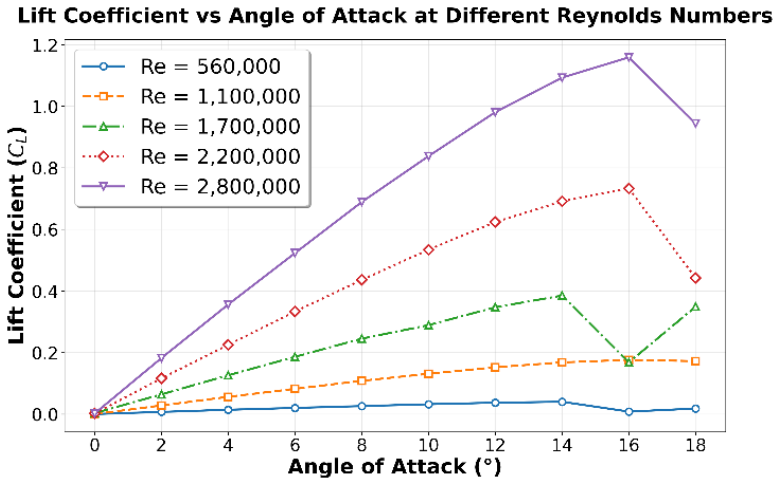


Figure 7. Curves showing the variation of C_L with attack angle at different Reynolds numbers. (picture credit : original)

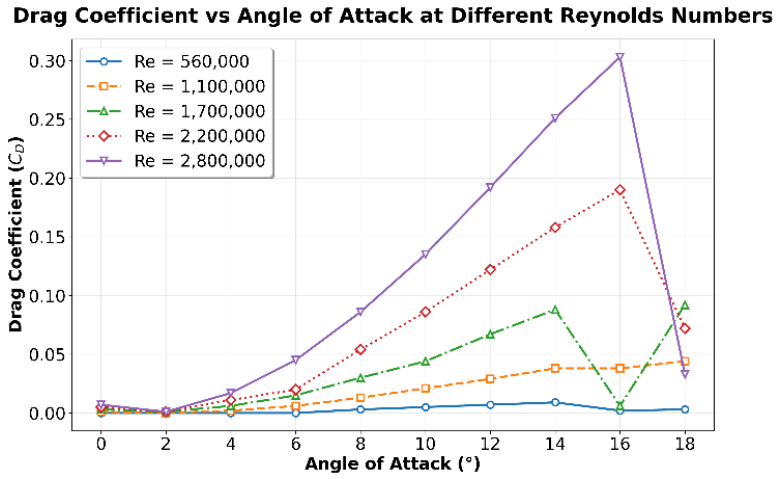


Figure 8. Curves showing the variation of C_D with attack angle at different Reynolds numbers. (picture credit : original)

DOI: 10.54254/2755-2721/2026.AD33186

4. Conclusion

The article is a systematic study of low Reynolds number regime (560, 000 -2, 800, 000) aerodynamic performance of NACA0012 airfoil under the CFD numerical simulation paradigm and the k - - left curly square SST turbulence model. The following were the conclusions:

1) They have found that the C_L of NACA0012 airfoil has a positive correlation with the Reynolds number within the studied range. The multiplication of the Reynolds number is a valuable delaying parameter of the separation of the flow field and the magnification of the lift-strengthening capability of the airfoil in the complex working conditions.

2) The C_L of the airfoil has a linear rise at the start and thereafter it decreases sharply with the rise in the AoA. The critical stall AoA of this airfoil is between 14 to 16 degrees in the current low Reynolds number environment and this is a reference point of the anti-stall design of small unmanned aircraft and low speed wind turbine blades.

In conclusion, the NACA0012 airfoil exhibits excellent flow controllability in low Reynolds number environments, but it is necessary to strictly control the operating AoA to avoid entering the deep stall zone.

References

[1] Molaa, A.A., Abdulwhaab, M. (2025) Numerical and experimental study of the impact on aerodynamic characteristics of the NACA0012 airfoil. Open Engineering, 14(1), 20220506.
[2] Jardin, T., Ferrand, V., Gowree, E.R. (2025) NACA0012 airfoil at Reynolds numbers between 50, 000 and 140, 000 — Part 1: Steady freestream. International Journal of Heat and Fluid Flow, 112, 109655.
[3] Rodríguez, I., Lehmkuhl, O., Borrell, R., Oliva, A. (2013) Direct numerical simulation of a NACA0012 in full stall. International Journal of Heat and Fluid Flow, 43, 194-203.
[4] Mohamad, F., & Yusri, M.Y. (2024). Computational Fluid Dynamics (CFD) Simulations of Wavy Leading Edge NACA0012 Wings. Journal of Aeronautics, Astronautics and Aviation, 56(1S), 477-485.
[5] Yu, Q., Hao, J. (2020) Dynamic Stall Simulation of NACA0012 Airfoil Based on Dynamic Grid. Computer Simulation, 37(4), 44-47+297.
[6] Goyaniuk, L., Poirel, D., Benaissa, A. (2020) Pitch–Heave Symmetric Stall Flutter of a NACA0012 at Transitional Reynolds Numbers, AIAA Journal 58(8), 3286-3298.
[7] Rak A, Grbčić L., Sikirica A., Kranjčević, L. (2023) Experimental and LBM analysis of medium-Reynolds number fluid flow around NACA0012 airfoil. International Journal of Numerical Methods for Heat & Fluid Flow, 33(5), 1955–1980.
[8] Wang, A., Lai, H. (2024) Control of separated flow at low Reynolds number around NACA0012 airfoil by boundary layer suction. J. Phys.: Conf. Ser. 2707, 012122
[9] Craik, A.D.D. Wave interactions and fluid flows. Cambridge University Press, Cambridge, England (1988).
[10] Navier, C. L. Navier stokes equation. Chez Carilian-Goeury, Paris, France (1838).